International Journal of Mechanical, Industrial and Aerospace Sciences
ISSN: 2517-9950
Vol:6, No:1, 2012

The Effect of Cyclone Shape and Dust Collector on Gas-Solid Flow and Performance

Kyoungwoo Park, Chol-Ho Hong, Ji-Won Han, Byeong-Sam Kim, Cha-Sik Park, and Oh Kyung Kwon

***Abstract*—**Numerical analysis of flow characteristics and separation efficiency in a high-efficiency cyclone has been performed. Several models based on the experimental observation for a design purpose were proposed. However, the model is only estimated the cyclone's performance under the limited environments; it is difficult to obtain a general model for all types of cyclones. The purpose of this study is to find out the flow characteristics and separation efficiency numerically. The Reynolds stress model (RSM) was employed instead of a standard k-ε or a k-ω model which was suitable for isotropic turbulence and it could predict the pressure drop and the Rankine vortex very well. For small particles, there were three significant components (entrance of vortex finder, cone, and dust collector) for the particle separation. In the present work, the particle re-entraining phenomenon from the dust collector to the cyclone body was observed after considerable time. This re-entrainment degraded the separation efficiency and was one of the significant factors for the separation efficiency of the cyclone.

***Keywords*—**CFD, High-efficiency cyclone, Pressure drop, Rankine vortex, Reynolds stress model (RSM), Separation efficiency.

I. Introduction

CYCOLNES, which can separate the particles from an air stream, have been widely used in many industrial processes, such as air pollution control and environmental cleaning processes due to their well adaptability to harsh conditions, simplicity to design, and low costs to operate and maintain. The cyclone designs are generally classified into straight-through, uni-flow, and reverse-flow cyclones according to the purpose in use. Among them, it is known that the use of tangential inlet and reverse-flow is the most common way for cyclone design.

Because of the above mentioned many merits of cyclone, much attention have been paid on predicting the flow fields in cyclones both by experimental and numerical methods for last few decades [1-3]. The performance of a cyclone separator is generally characterized by the collection efficiency of particles and the pressure drop through the cyclone. According to the many researches, the cyclone height, diameter, and shape (i.e., cylinder or rectangular), the shape and diameter of vortex finder, and the inlet geometry can influence considerably the performance of the cyclones.

Kyoungwoo Park is with the Department of Mechanical Engineering, Hoseo University, Asan 336-795, Rep. of Korea (phone:+82-41-540-5804; fax: +82-41-540-5808; e-mail: kpark@hoseo.edu).

Chol Ho Hong is with the Department of System Control Engineering, Hoseo University, Asan 336-795, Rep. of Korea (e-mail: chhong@hoseo. edu).

Ji Won Han is with the Department of Mechanical Engineering, Hoseo University, Asan 336-795, Rep. of Korea (e-mail: jwhan@ hoseo. edu).

Byeong Sam Kim is with the Department of Automotive Engineering, Hoseo University, Asan 336-795, Rep. of Korea (e-mail: kbs@ hoseo. edu).

Oh Kyung Kwon is with the KITECH, Cheonan 330-825, Rep. of Korea (e-mail: kwonok@kitech.re.kr)

In 2006, [4] analyzed the influence of the shape of the cyclone cylinder on the flow characteristics and collection performance by using the commercial package, FLUENT. They observed that the long-cone cyclone has an unstable flow fields and these characteristics results in the short circulating flow at the vortex finder opening and affects adversely the particle collection efficiency.

[5] evaluated the effect of vortex finder shape and diameter on cyclone performance and flow field numerically. In order to predict particles tracking in the cyclone, the Eulerian-Lagrangian procedure was used. They found that the tangential velocity and separation efficiency are decreased when the cyclone vortex finder diameter is increased.

Recently, [6] studied numerically the effect of cyclone inlet dimension on the flow pattern and performance using the Reynolds stress turbulence model (RSM) for five cyclone separators. They showed that the tangential velocity in the cyclone decreases with increasing the cyclone inlet dimensions. They also found that the effect of changing the inlet width is more significant than that of the inlet height for the cut-off diameter and the optimal ratio of inlet width to height, b/a, is from 0.5 to 0.7.

The interaction of gas-solid plays an important role in the flow field and performance in cyclones. There are two kinds of methods to predict it, that is, one-way and two-way coupling approaches. An one-way coupling method is base on the assumption that the presence of the particles doses not affect the flow field because the particle loading in a cyclone separator is small [7]. On the contrary, a two-way coupling effect [8] is considered the effect of the particles on the gas flow. In this model, the particle source-in cell (PSIC) model is generally used to solve the momentum equation of a particle in the two-phase flow.

In the present study, the effects of the cyclone dimensions, the particle size, and the presence of dust collector on the flow characteristics and performance of the cyclone are investigated numerically. The turbulent flow is analyzed by using the Reynolds stress model (RSM) and the Eulerian-Lagrangian approach is implemented for predicting the particle motion. A one-way coupling effect, which the gas flow is not affected by the presence of the particles, is employed to estimate the gas-solid interaction. The computational model can predict the two-phase flow in cyclones accurately and provide the design concept for the presence of the dust collector.

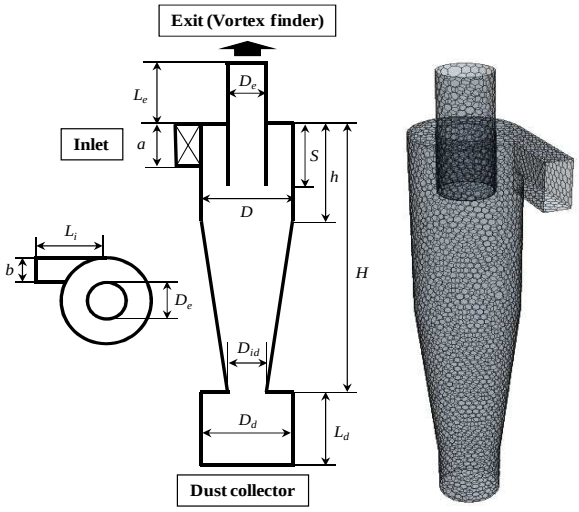

Fig. 1 Schematics of the cyclone and its grid system

II. Physical Model

The schematic of the cyclone separator and the generated grid system considered in the present work is given in Fig. 1 and the geometrical dimensions are depicted in Table 1. As can be seen in Table 1, all dimensions are normalized by using the diameter of cyclone body (D = 290 mm). According to the cyclone's height, it can be divided into three parts such as vortex finder (annular space), separation space and dust collection part. The inlet pipe is mounted tangentially onto the side of the cylindrical part of the cyclone body and the working fluid (gas and particles) is incoming through this section with the uniform velocity such as v_{in} = 25 *m/s*. The exit tube, called the vortex finder, is fixed on the top of the cyclone.

III. Theoretical Analysis

A. Governing Equations

The flow in cyclones is assumed to be turbulent swirl flow with incompressible fluid and it can be reasonably predicted by the Reynolds stress model (RSM). The turbulent flow for gas can be described by the Reynolds-Average Navier-Stokes (RANS) equation and the equation of continuity for the mean motion. They are expressed in tensor notation as follows:

TABLE I
Geometrical Dimensions For The Cyclone

Dimension	Values/ D (mm)
Cyclone diameter (D)	1.0D (290 mm)
Gas outlet diameter (D_e)	0.5D (145 mm)
Dust collector inlet diameter (D_{id})	3/8D (108 mm)
Dust collector diameter (D_d)	1.0D (290 mm)
Exit length (L_e)	2.0D (580 mm)
Vortex finder length (S)	0.5D (1245mm)
Cylinder length (h)	0.5D (145 mm)
Cyclone length (H)	4.0D (1160 mm)
Dust collector length (L_d)	1.7D (493 mm)
Inlet width (a)	0.2D (58 mm)
Inlet height (b)	0.5D (145 mm)
Inlet length (l)	1.0D (290 mm)

$$\frac{\partial}{\partial x_i}(U_i) = 0 \tag{1}$$

$$\frac{\partial}{\partial t}(U_i) + U_j \frac{\partial U_i}{\partial x_j} = -\frac{1}{\rho}\frac{\partial P}{\partial x_i} + \nu \frac{\partial^2 U_i}{\partial x_i \partial x_j} - \frac{\partial}{\partial x_j}\left(\overline{u_i' u_j'}\right) \tag{2}$$

Where U_i is the mean velocity, x_i the coordinate system, t the time, P the mean pressure, ρ the gas density, and ν the kinematic viscosity. $\overline{u_i' u_j'}$ (= R_{ij}) represents the Reynolds stress tensor and $u_i' = u_i - U_i$ is the i-th fluid fluctuation velocity component. As shown in Eq.(2), the Reynolds stresses should be modeled using various assumptions. In the present work, the Reynolds stress terms are directly calculated by RSTM.

B. Turbulent Modeling

The accurate prediction of a strong turbulent swirl flow is generally dependent on the turbulent model used. In the present work, the Reynolds stress turbulent model (RSTM) which solves the individual Reynolds stress term ($-\overline{u_i' u_j'}$) by using differential transport equations is used. The transport equations of Reynolds stresses can be written as

$$\frac{\partial}{\partial t}\left(\overline{u_i' u_j'}\right) + \frac{\partial}{\partial x_k}\left(U_k \overline{u_i' u_j'}\right) = D_{ij} + P_{ij} + \Pi_{ij} + E_{ij} \tag{3}$$

Where the individual terms in the right hand side stand for stress diffusion, stress production, pressure strain, and dissipation terms, respectively, and defined as follows;

$$D_{ij} = \frac{\partial}{\partial x_k}\left(\frac{\nu_t}{\sigma_k}\frac{\partial}{\partial x_k}\left(\overline{u_i' u_j'}\right)\right) \tag{4}$$

$$P_{ij} = -\left[\overline{u_i' u_k'}\frac{\partial U_j}{\partial x_k} + \overline{u_j' u_k'}\frac{\partial U_i}{\partial x_k}\right], \quad P = \frac{1}{2}P_{ij} \tag{5}$$

$$\Pi_{ij} = -\left[C_1 \frac{\varepsilon}{k}\left(\overline{u_i' u_k'} - \frac{2}{3}\delta_{ij}k\right) + C_2\left(P_{ij} - \frac{2}{3}\delta_{ij}P\right)\right] \tag{6}$$

$$E_{ij} = -\frac{2}{3}\delta_{ij}\varepsilon \tag{7}$$

Here ν_t is the turbulent viscosity, P the fluctuation kinetic energy production, k the turbulent kinetic energy ($= (1/2)\overline{u_i' u_j'}$), and ε the dissipation rate of k, respectively. The empirical constants are $\sigma_k = 1$, $C_1 = 1.8$, and $C_2 = 0.6$ [9].

The transport equation for the turbulent dissipation rate (ε) is expressed as

$$\frac{\partial \varepsilon}{\partial t} + U_j \frac{\partial \varepsilon}{\partial x_j} = \frac{\partial}{\partial x_j}\left[\left(\nu + \frac{\nu_t}{\sigma_\varepsilon}\right)\frac{\partial \varepsilon}{\partial x_j}\right] - C_{\varepsilon 1}\frac{\varepsilon}{k}\left(\overline{u_i' u_j'}\right)\frac{\partial U_i}{\partial x_j} - C_{\varepsilon 2}\frac{\varepsilon^2}{k} \tag{8}$$

The values of constants are $\sigma_\varepsilon = 1.3$, $C_{\varepsilon 1} = 1.44$ and $C_{\varepsilon 2} = 1.92$.

C. Particle Motion Equations

The basic assumptions employed in the present work to model the particle motion are as follows; the solid (particle) has a fully spherical shape and disperses dilutely in the gas phase so that the gas-solid interactions and the influence of the dispersed particle volume fraction on the gas phase are negligibly small.

Generally, the particle loading in a cyclone is small (3 - 5%), and therefore, it can be assumed that the presence of the particles does not affect the flow field (i.e., one-way coupling). Additionally, collisions between particles and the walls of the cyclone are assumed to be perfectly elastic and the interaction between particles is neglected because of dilute flow. In order to simulate the particle motion in the cyclone, the discrete phase model (DPM) was used by defining the initial position, velocity and size of individual particles. The trajectory of particles was obtained by integrating the force balance on the particle. The equation of motion of a small particle, which is included the effects of nonlinear drag and gravitational forces, in terms of the Eulerian-Lagrangian approach is given by [10].

$$\frac{du_{p,i}}{dt} = \frac{18\mu}{\rho_p d_p^2}\frac{C_D \mathrm{Re}_r}{24}\left(u_i - u_{p,i}\right) + g_i \cdot \left(1 - \frac{\rho}{\rho_p}\right) \quad (9)$$

$$\frac{dx_{p,i}}{dt} = u_{p,i} \quad (10)$$

Here u_i and $u_{p,i}$ are the gas and particle velocities in i-direction, respectively, $x_{p,i}$ its position, ρ_p the particle density, d_p the particle diameter, g_i the acceleration of gravity in i-direction. ρ, μ are the density and viscosity of gas, respectively. Re_r represents the relative Reynolds number, which is defined as

$$\mathrm{Re}_r = \frac{\rho d_p \left|u_{p,i} - u_i\right|}{\mu} \quad (11)$$

The drag coefficient, C_D, for spherical particles is calculated by using the correlation proposed by Hinds[11]

$$C_D = \frac{24}{\mathrm{Re}_r} \quad \text{for } \mathrm{Re}_r < 1 \quad (12)$$

$$C_D = \frac{24}{\mathrm{Re}_r}\left(1 + \frac{1}{6}\mathrm{Re}_r^{2/3}\right) \quad \text{for } 1 < \mathrm{Re}_r < 400 \quad (13)$$

The first term on the right-hand side (RHS) of Eq.(9) is the drag force per unit particle mass, generally the dominating force, due to the relative slip between the particle and the fluid.

D. Numerical Approaches

The gas phase is treated as a continuum by solving the RNS equations with the turbulent model, while the solid (or disperse) phase is solved by tracking a large number of particles through the calculated flow field. The dispersed phase can exchange mass, momentum, and energy with the fluid phase. The numerical simulations presented in this work were done by means of STAR-CCM+ [12] which is one of the general purpose commercial S/Ws. The pressure-velocity coupling problem is resolved by the SIMPLE algorithm [13]. The unsteady RSTM was used with a time step of 0.0001s. Due to difficulty to reach the convergence in simulations, the standard $k-\varepsilon$ model was used firstly to calculate the turbulent properties, and then the RSTM was adopted to obtain the final results. The solutions are treated as converged ones when the sum of normalized residual is less than 1×10^{-5}.

The boundary condition for airflow velocities at the cyclone inlet was assumed to be uniform at different inlet velocities. The pressure boundary condition at exit was employed. At the wall, no-slip boundary condition was applied for velocity.

IV. Results and Discussion

A. Validation of CFD Model in the Cyclone

Fig. 2 presents the pressure drop in the cyclone separator for various inlet velocities in order to validate the present CFD-model by comparing the experimental data and the computational results [14]. As shown in this figure, the pressure drop calculated in the present work shows a good agreement with the experimental data. It can be also seen that the pressure drop, which is strongly related with the pumping power, increases with the increase of the inlet velocity.

B. Comparison of Turbulent Models

Comparison of tangential velocity profiles calculated at y = -0.4m using the RSTM and standard $k-\varepsilon$ model are shown in Fig. 3. As can be seen, the RSTM predicts much better compared to the other model. The highly swirl flow, in general, generates a strong anisotropy in the turbulent structure and it causes the standard $k-\varepsilon$ model to provide inaccurate prediction of both the location of maximum velocity and the Rankine vortex which is composed of a forced vortex(inner region near the cyclone axis) and a free vortex(near the wall). It is clear that the RSTM model can predict the Rankin-type tangential velocity profiles very well.

C. Grid Dependency

Grid refinement test has been performed in order to make sure that the solutions are grid independent. For this, three grid systems (i.e., the number of 120,000, 250,000 and 420,000) are generated and compared with each of them for non-dimensional axial velocity (v_a/v_{in}) in Fig. 4 and computational time in Table II. The polyhedral mesh with high-aspect layer method is used to generate the grid systems because the high-pressure gradient and strong double vortex flow (swirl

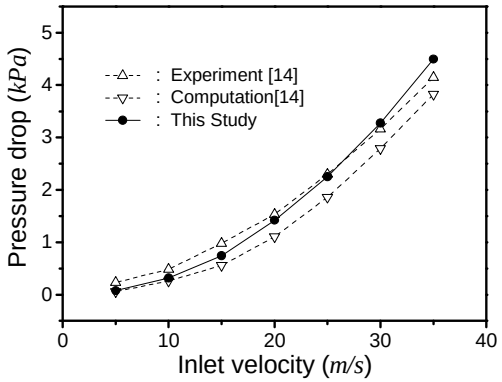

Fig. 2 Validation of computational model by comparison with the experimental data [14]

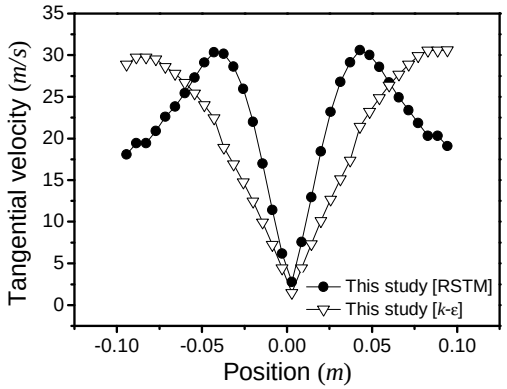

Fig. 3 Comparison of turbulent models at v_{in} = 25 *m/s*

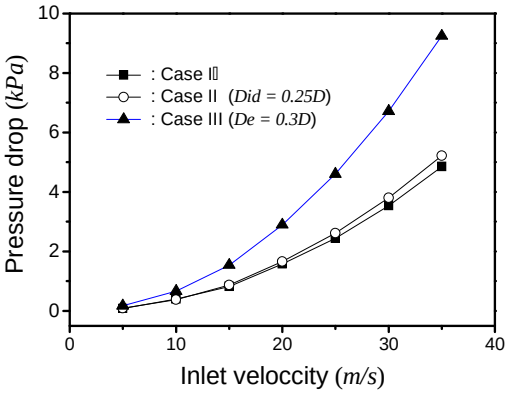

Fig. 5 Pressure drop according to inlet velocity for various cyclone specifications

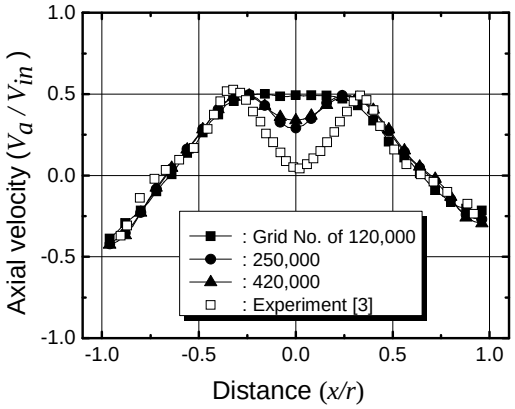

Fig. 4 Grid dependency for three cases of grid systems

TABLE II
COMPUTATIONAL TIME FOR THREE GRID SYSTEMS

	Base	Refine #1	Refine #2
No. of cells	120,000	250,000	420,000
Computational time (hours)	5.5	12.5	22.0

flow) are occurred in the cyclone. As shown in Fig. 4, the axial velocity profiles have a good agreement with the experimental data [3] except for the base grid (120,000). Table II shows the computational time for three grid systems and Refine #3 (No. of 420,000) needs more time to convergence. In the present work, all computational results are obtained using the 250,000 cells grid by considering both the accuracy and the computational cost.

D. Flow Characteristics

The performances of the cyclone are the separation efficiency and pressure drop. It is well known that the increase of inlet velocity of gas can increase both the pressure drop and separation efficiency, simultaneously. In the present work, the effects of inlet gas velocity and cyclone shape on the pressure drop are investigated firstly. Fig. 5 shows the pressure drop in the cyclone according to the inlet velocity for three cases. It can be seen in this figure that increasing the inlet velocity causes the pressure drop to increase exponentionally. In addition, the vortex finder diameter (CASE III, D_e = 0.5D → 0.3D) greatly affects the pressure drop compared to that of con tip diameter (CASE II, D_{id} = 3/8D → 0.25D) at the same inlet velocity as shown in Fig. 6. This means that the effect of D_e on the cyclone performance (pressure drop) is much significant than that of D_{id}. It is also found that the con tip diameter has almost no influence on pressure drop and the effect of vortex finder diameter on the pressure drop becomes significantly as the inlet velocity is increased. From this result, it is necessary to carry out the optimization for the cyclone shape.

E. Separation Efficiency

The separation efficiency (η), which is one of the cyclone performances, is defined as follows [15],

$$\eta = 1 - \exp\left[-\frac{\rho_p}{9\mu}\left(\frac{2d_p v_t}{D}\right)^2 t_{res}\right] \quad (14)$$

where t_{res} is the gas residence time in the cyclone and it includes following two parts:

$$t_{res} = \frac{V_{in}}{Q} + \frac{1}{0.9}\frac{V_s}{Q} \quad (15)$$

In the right hand side of Eq.(15), the first and second terms represent the mean gas residence time in the entry region and in the outer vortex, respectively. V_{in} is the volume of the entry region below the centerline of the inlet duct and Q is the volumetric gas throughout. Especially, V_s is defined due to the fact that about 90% of the entire inlet gas volume flows from the outer vortex to the inlet vortex core along the cyclone wall. More detailed equations for them are explained in [16]. In the present work, the particle residence time for three cases, which is an important factor for predicting the separation efficiency, is calculated fort the inlet velocity of 25 m/s and they are listed in Table III.

Fig. 6 presents the separation efficiency for various inlet velocities. As shown in Fig. 6, η is increased with the inlet velocity and this is a general phenomenon in cyclones. It can be also seen from the figure that the cut-off size (x_{50}), which is one of the fundamental characteristics of cyclones, is varied with the particle diameter. The meaning of x_{50} is the diameter of particle that has a 50% probability of capture by the spin of the inner vortex. For low mass loading, the cut-off size can be defined as follows [17],

TABLE III
PARTICLE RESIDENCE TIME IN EQ. (12)

CASE I	3.16 (sec)
CASE II	6.05 (sec)
CASE III	7.78 (sec)

$$x_{50} = \sqrt{\frac{18\mu(0.9Q)}{2\pi(\rho_p - \rho)v_{t,cs}(H_t - S)}} \quad (16)$$

where $v_{t,cs}$ is the tangential velocity of the gas at the inner core radius and H_t represents the cyclone total height.

As can be seen in Fig. 6, the values of cut-off size are predicted according to the inlet velocity, that is, the particle sizes of x_{50} are $2.5\mu m$, $1.8\mu m$, and $1.5\mu m$ for $v_{in} = 10$, 15, and 20 *m/s*, respectively. It is also found that if the particle diameter is over $4\mu m$; all particles are separated irrespective of the inlet velocity. The particles which are entered at inlet are moved with the gas phase and if the centrifugal force is strongly enough, they are pushed the outside of CS (control surface, a virtually extended surface of the vortex finder) and falling along the cyclone wall and then collected at the dust collector. However, small particles, which generally flow with a gas because of a weak centrifugal force, enter the inside of CS and then outflow through exit.

Figure 7 shows the existence amount of solid particle inside the cyclone at a specific time. It can be found that the amount solid particle is decreased with pass by time except for a heavy particle such as a particle diameter of $3\mu m$. This means that small particles flow out with a gas. In addition, Figure 7 also shows that the fractional efficiency is abruptly decreased at a certain time. This is due to the fact that the particle in the cyclone outflows through three different flow passages during its downward movement : (1) some particles leave the cyclone through the entrance of the vortex finder as soon as the particle enters inside the cyclone, (2) the second passage is that the particle outflows with a gas flow from the end of con-tip after time passes a little bit, (3) for the cases of $d_p < 1.75\mu m$ (i.e., light particles), the fractional efficiency is dramatically decreased within several seconds. The particles with small diameter flow into the dust corrector and most of them are flow out from the corrector because of a small quantity of moment of gas in the dust corrector while the large particle is remained at the corrector.

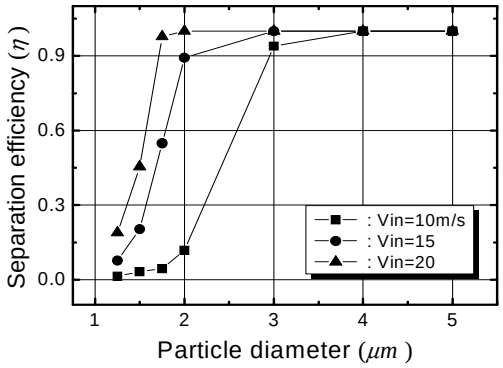

Fig. 6 Separation efficiency according to the particle diameter for various inlet velocities

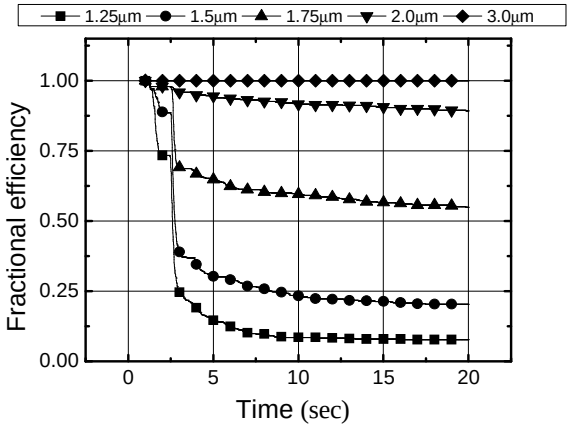

Fig. 7 Fractional efficiency according to the time for various particle diameters

Fig. 8 shows the separation efficiency for various particle diameters and cyclone shape. For the same particle diameter, the separation efficiency is greater than that of base model (CASE I). In addition, when the particle diameter is larger than 5 μm, there is no influence on the efficiency irrespective of the cyclone shape as shown in Fig. 8. Figure 8 also shows that the diameter of the con tip (CASE II, $D_{id} = 0.25D(72.5mm)$) and vortex finder (CASE III, $D_e = 0.3D(57mm)$) has a significant

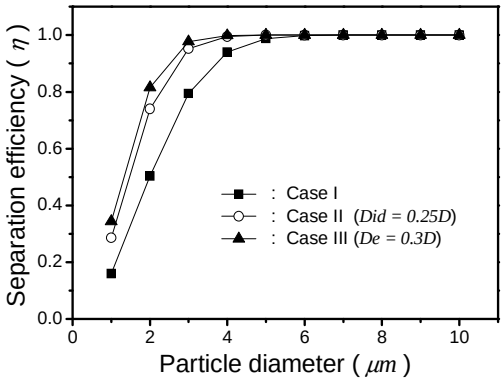

Fig. 8 Separation efficiency according to the particle diameter for various cyclone specifications

influence on the efficiency compared to the base model (CASE I) while the effect of it on the pressure drop is slight, as explained in Fig. 5. It is also found from Fig. 5 and Fig. 8 that higher tangential velocity results in larger centrifugal force, which in turn leads to higher separation efficiency. An interesting fact is found between Fig. 5 and Fig. 8 that the pressure drop inside the cyclone is little influenced by the con tip diameter (D_{id}), whereas it greatly affects on the cyclone efficiency. This means the con tip diameter is most significant factor from the performance point of view in the cyclone design.

V. Conclusions

In order to obtain the optimal solutions of the design variables of the cyclone separator, the effect of diameters of vortex finder and cone tip diameters on its performance such as separation efficiency and pressure drop were numerically carried out. For this, the cost effective and high fidelity RANS solver for turbulent flow such as the commercial software (i.e., STAR-CD) was used. Reynolds stress transport model (RSTM) was adopted to simulate the anisotropic turbulent flow in a cyclone and this model had a good agreement compared with the experimental data. As the results of the present work, the effect of vortex finder diameter (D_e) on the performance was much greater than that of con tip diameter. It could be also found that the diameter of the con tip (B) has significant influence on the efficiency while it has almost no influence on the pressure drop. That is, from the performance of cyclone point of view, the con tip diameter is more significant parameter than the vortex finder diameter. Due to the tradeoffs between the conflicting objective functions (i.e., pressure drop and separation efficiency), the shape optimization has to be carried out in our further study.

Acknowledgment

This work was supported by the New and Renewable Energy of the Korea Institute of Energy Technology Evaluation and Planning (KETEP) grant funded by the Korea government Ministry of Knowledge Economy (No. 2010T100100850).

Nomenclature

k Turbulent kinetic energy
P_{ij} Turbulent production term
$\triangle p$ Pressure drop
U_i Mean velocity component
u_i' Fluctuation component of *i*-direction
$\overline{u_i'u_j'}$ Reynolds stress term
v_t Tangential velocity
x_i Coordinate system
ε Dissipation rate of k
η Separation efficiency in Eq.14
μ Viscosity
ν_t Turbulent eddy viscosity
ρ Gas density
ρ_p Particle density

References

[1] D. Leith, W. Licht, the Collection Efficiency of Cyclone Type Particle Collectors-A New Theoretical Approach, *AIChE Symp*. Ser. 68, pp.196-206, 1972.
[2] A.J. Hoekstra, H.J Derksen, H.E.A. Van Den Akker, An Experimental and numerical study of turbulent swirling flow in gas cyclones, *Chem. Eng. Sci*. Vol.54, pp.2055-2065, 1999.
[3] A.J. Hoekstra, *Gas flow field and collection efficiency of cyclone separators*, Ph.D. Thesis, Technical University Delft, 2000.
[4] J.W. Lee, H.J. Yang, and D. Y. Lee, Effect of cylinder shape of a long-coned cyclone on the stable flow-field establishment, *Powder Technology*, Vol.165, pp.30-38, 2006.
[5] A. Raoufi, M. Shams, M. Farzaneh, and R. Ebrahimi, Numerical simulation and optimization of fluid flow in a cyclone vortex finder, *Chemical Engineering and Processing*, vol. 47pp. 128-137, 2008.
[6] K. Elsayed and C. Lacor, The effect of cyclone inlet dimensions on the flow pattern and performance", *Applied Mathematical Modeling*, vol.35, pp. 1952-1968, 2011.
[7] J.J. Derksen, Separation performance predictions of a Stairmand high efficiency cyclone, *AIChE Journal*, Vol.49, pp.1359-1371, 2003.
[8] G. Wan, G. Sun, X. Xue, and M. Shi, Solid concentration simulation of different size particles in a cyclone separator, *Powder Technology*, vol. 183, pp.94-104, 2008.
[9] B.E. Launder, G.J. Reece, and W. Rodi, Progress in the development of a Reynolds stress turbulent closure, *J. of Fluid Mechanics*, vol.68, pp. 537-538, 1975.
[10] B. Zhao, Y. Su, and J, Zhang, Simulation of gas flow pattern and separation efficiency in cyclone with conventional single and spiral double inlet configuration, *Chemical Engineering Research and Design*, vol.84, pp.1158-1165, 2006.
[11] W.C. Hinds, *Aerosol Technology: Properties Behavior and Measurement of Airborne Particles*, John Wiley & Sons, New York, 1982.
[12] STAR-CCM+ v4.02 Methodology, 2007.
[13] S.V. Patankar, *Numerical Heat Transfer and Fluid Flow*, Taylor & Francis, 1980.
[14] B. Wang, L.L. Xu, K.W. Chu, and A.B. Yu, Numerical study of gas-solid Flow in a Cyclone Separator, *Applied Mathematical Modeling*, vol.30, pp.1326-1342, 2006.
[15] R. Clift, M. Ghadiri and A.C. Hoffman, A Critique of two models for cyclone performance, *AIChE Journal*, vol.37, No.2, pp.285-289, 1991.
[16] F. Qian, M. Zhang, An Extended model for determining the separation performance of a cyclone, *Chem. Eng. Technol*, vol.29, no.6, pp.724-728, 2006.
[17] A.C. Hoffman and L.E. Stein, *Gas Cyclones and Swirl Tubes:Principles , Design, and Operation*, 2nd Ed. Springer, 2008.

Kyoungwoo Park: Dr. Kyoungwoo Park is currently working at Department of Mechanical Engineering in Hoseo University as a professor. As soon as he acquired his Ph.D. degree at Hanyang University, he entered the LG Industrial Systems Co., Ltd., and he researched on the flow and thermal characteristics around/in elevators. In 1999, he joined the Ralph Greif research team for two and half years, who is a professor of University of California at Berkeley and studied about convection heat transfer with CFD. After he came back to Korea in 2001, he researched and taught students at IDOT of Hanyang University until Feb. 2005. His main interesting fields are heat transfer, micro/macro thermo/ fluid dynamics, optimization, and CFD. Recently, his researches are focus on the semiconductor and display manufacturing process and the aerodynamics and optimization of Wing-In- Ground Effect Vehicles.